# Microscopic Cluster Formation during the Laser Desorption of Chrysene-$d_{12}$

**Steven M. Hankin and Phillip John***

*Department of Chemistry, Heriot-Watt University, Riccarton, Edinburgh EH14 4AS, U.K.*

*Received: March 17, 1999*

The laser ablation of chrysene-$d_{12}$ has been investigated by laser desorption/post-ionization time-of-flight mass spectrometry (L2ToFMS). The early stages of plume expansion were probed by locating the focus of the post-ionization laser to within 50 $\mu$m of the surface. A spatial and temporal study of the desorption plume was carried out by recording positive ion time-of-flight mass spectra as a function of delay time and position. When the ionization laser focus was moved to within 50 $\mu$m of the surface, the appearance of the chrysene-$d_{12}$ parent ion signals changed from being sharply defined with a mass resolution of ~700 to broad signals of reduced intensity and a significantly lower resolution. Furthermore, the broad ionization signals were observed at longer delay times on increasing the desorption laser power. We attribute the observed phenomena to the laser desorption of molecular clusters, their transient survival, and ultimate evaporation to discrete molecules.

## Introduction

A detailed understanding of the mechanism of high power pulsed laser desorption of molecules has not emerged despite a considerable number of theoretical[1−7] and experimental[8−18] studies. Extensive experimental studies of laser ablation plumes have been conducted using a variety of techniques including laser-induced fluorescence imaging,[19−21] post-ionization using X-rays[22] or focused lasers[9,11−13,15−18] coupled with time-of-flight mass spectrometry. Recent molecular dynamics studies[1−3] have predicted the presence of clusters as well as discrete molecules within the evolving plume. Conventionally, desorption plumes resulting from high power laser irradiation of solids have been imaged at distances extending to several centimeters[19−21] from the surface. However, these studies preclude probing the initial stages of plume evolution occurring close to the surface.

In the present study, the ability to locate the post-ionization laser focus as close as 50 $\mu$m to the surface with a precision of $\pm$10 $\mu$m has allowed experiments to be conducted on monitoring collisional processes within the desorption plume. Two-laser time-of-flight mass spectrometry (L2ToFMS) has been employed to probe the desorbed plume generated from the laser irradiation of the polyaromatic hydrocarbon chrysene-$d_{12}$. We report on laser ionization mass spectral observations of phenomena which can be attributed to the presence of molecular clusters within the expanding laser generated plume.

## Experimental Section

The construction of the L2ToF mass spectrometer has been described previously.[23,24] Alignment of the desorption and ionization lasers with respect to the surface of the sample was achieved by viewing the fluorescence from laser irradiation of a thin layer of chrysene-$d_{12}$ (98 atom % D purity; Aldrich, Gillingham, U.K.) using an optical microscope (Olympus, BH2-DO) attached to a color video camera (Hitachi, VK−C150ED). Movement of the samples on the *x*, *y* and *z*-axes of the rotary sample stage was achieved using precision translation micrometers. The sample was translated relative to the fixed desorption laser. The ionization laser focus could be positioned >30 $\mu$m above the sample using the micrometer translation stage of the focusing lens. The focus was translated in the direction of the desorbing molecules (*z*-axis), parallel to the sample surface, to spatially profile the desorption plume of chrysene-$d_{12}$ neutral molecules. The area profiled extended to 300 $\mu$m from the point of desorption in the $x-y$ plane and from 30 $\mu$m to 600 $\mu$m along the ion axis. The fourth harmonic output (266 nm, 10 ns pulse width, 1 Hz) of a Nd:YAG laser (Quanta-Ray DCR-11, Spectra-Physics) was used for desorption. Achromatic focusing of the desorption beam to a spatial resolution of 1−2 $\mu$m normal to the sample surface was accomplished using a Cassegrain reflecting objective lens (focal length = 14 mm). The desorbed neutrals were ionized at 266 nm using a 10 ns pulse from a second Nd:YAG laser (Quanta-Ray DCR-11, Spectra-Physics; <10 $\mu$J pulse$^{-1}$). The beam was focused within the ablation plume using a fused silica UV-grade biconvex lens (focal length = 150 mm, diameter = 25 mm). The beam waist at the focus of the ionization laser was estimated to be ca. 15 $\mu$m. Synchronous firing of the two Nd:YAG lasers was controlled using a variable time delay unit (0−50 ms with a jitter of <20 ns). The chrysene-$d_{12}$ parent ion peak intensity at *m*/*z* 240 was measured as a function of the delay time between the desorption and ionization pulses. Spectra were collected after establishing signal uniformity for ~50 single shots at 1 Hz. The post ionization signal was contingent on the presence of both laser pulses; removal of either eliminated the signal. The ions were mass separated (nominal mass resolution $m/\Delta m$ = 700 at *m*/*z* 240) using a 2 meter flight tube fitted with a reflectron. The ions were detected by a dual microchannel plate (Galileo 3025MA) detector capable of operation from 2 to 20 kV. The amplified signal was fed to a 175 MHz transient digitizer (LeCroy 9400A) and transferred to a PC for display and analysis.

Chrysene-$d_{12}$ was used without further purification. The thin film of chrysene-$d_{12}$, used for alignment of the desorption and ionization laser beams, was prepared by depositing 50 $\mu$L of a solution of chrysene-$d_{12}$ ($8 \times 10^{-4}$ mol dm$^{-3}$, HPLC grade toluene) onto an aluminum stub and evaporating the solvent at room temperature. Samples for laser desorption studies were prepared from a suspension of chrysene-$d_{12}$ in 250 $\mu$L of HPLC

* E-mail: p.john@hw.ac.uk. Fax: +44 (0)131 451 3180.

10.1021/jp990950a CCC: $18.00 
Published on Web 05/13/1999

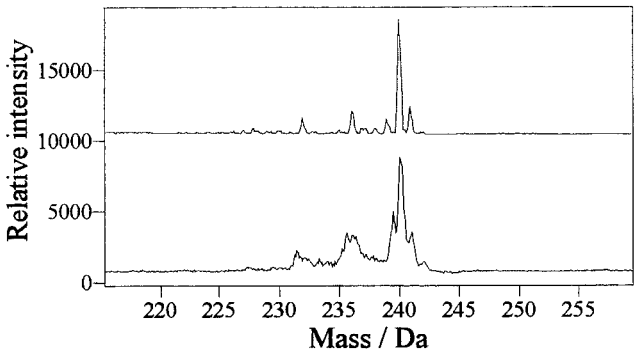


**Figure 1.** L2ToF mass spectra of laser-desorbed chrysene-$d_{12}$ recorded at (a) 100 $\mu$m and (b) 50 $\mu$m from the surface for a fixed delay of 0.4 $\mu$s between desorption and ionization. The desorption laser power density was 15 MW cm$^{-2}$ at 266 nm with a spatial resolution of 1 $\mu$m. Minor peaks corresponding to [M-$n$H] where $n = 1-5$ are associated with the 2 atom % H present in the chrysene-$d_{12}$.

grade toluene. Isolated microcrystallites of chrysene-$d_{12}$ adhered to an aluminum stub following deposition and evaporation of the solvent at room temperature. The samples were subsequently placed in a turbomolecular pumped load-lock ($10^{-7}$ Torr) to remove the final traces of solvent prior to entry into the main chamber.

## Results

A single, isolated, chrysene-$d_{12}$ crystallite (20 $\mu$m dia.) was optically imaged using the high-magnification video-microscope and irradiated at a spatial resolution of 1 $\mu$m at 266 nm. The mass spectra, recorded with an ionization laser energy $<10$ $\mu$J pulse$^{-1}$, comprised signals exclusively due to the chrysene-$d_{12}$ parent ion envelope, as shown in Figure 1a. The ion signals arose from desorption from the crystallite and precluded desorption remote from the defined site. The observed flight time for the chrysene-$d_{12}$ molecular ion ($m/z$ 240) is $\sim$73 $\mu$s. Signals were obtained as a function of delay time at a fixed sample ionization distance of 200 $\mu$m. The maximum signal intensity was observed at 0.4 $\mu$s delay at a desorption power density of 15 MW cm$^{-2}$. The maximum delay time at which post-ionization signals could be observed with S:N > 3:1 was $\sim$2 $\mu$s. Ion signals were not observed at delay times greater than 2.0 $\mu$s. The signal intensity at $m/z$ 240 was recorded as a function of distance, in increments of 25 $\mu$m, at a fixed time delay (0.4 $\mu$s) between the desorption and ionization pulses.

The parent ion envelope altered in appearance when the ionization focus was moved to within $\sim$50 $\mu$m of the surface at a desorption laser power density of 15 MW cm$^{-2}$. As shown in Figure 1a and b, the parent ion envelope peaks changed from being sharply defined with a mass resolution of $\sim$700 to a broad signal of reduced intensity and a significantly lower resolution. The phenomenon was not observed for distances that were greater than $\sim$50 $\mu$m from the surface at the lowest power density employed (15 MW cm$^{-2}$). Ion signals were not observed in the absence of the desorption laser, confirming that all ion signals arose from the post-ionization of desorbed neutral molecules and not from the ionization laser grazing the sample surface.

This phenomenon was further investigated by spatially and temporally probing the laser desorbed plume. First, with the ionization focus positioned 50 $\mu$m away from the surface, the range of delay times over which the effect was observed was found to be $\sim$0.2$-$0.3 $\mu$s at 15 MW cm$^{-2}$. High-resolution mass spectra, identical to Figure 1a, were always observed at delay times greater than 0.4 $\mu$s. Second, at a fixed distance of 100 $\mu$m away from the surface, the temporal limits of the effect were monitored as a function of desorption laser power. Figure 2 illustrates the average delay time limits when either poor resolution peaks or sharply resolved peaks could be observed as a function of increasing desorption laser power.

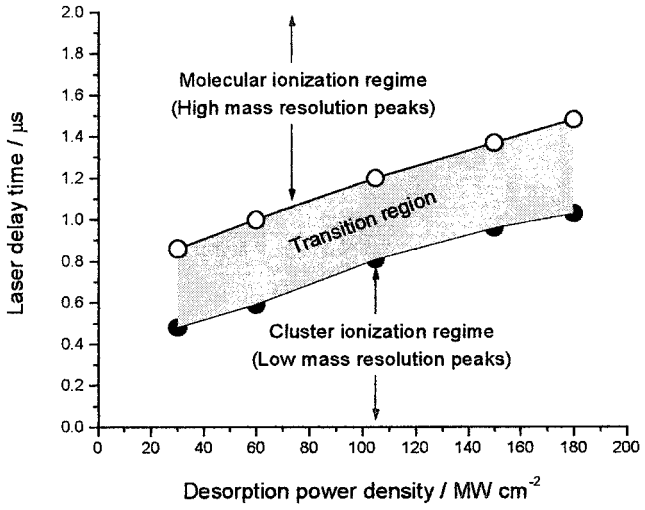


**Figure 2.** Dependence of the desorption power density on the temporal limits of the molecular and cluster ionization phenomena. The ionization focus was located 100 $\mu$m from the surface.

## Discussion

A molecular dynamics study of the laser desorption of organic solids has recently been reported by Garrison et al.[1−3] A number of novel features of the ablation process has been predicted including the presence of molecular clusters in the desorption plume. The rapid transfer of the desorption laser energy into the thermal energy of the crystal results in a sharp temperature rise within the pulse duration. Rapid melting in the surface layers of the sample causes expansion of the superheated liquid leading to explosive ejection. The resulting plume consists of molecular clusters or minuscule liquid droplets of various sizes in addition to the discrete molecules, as shown in Figure 3. The droplets do not vaporize rapidly to individual molecules but remain as a major component of the ejected plume for a period of $\sim$1 ns after the 15 ps desorption pulse. This model related the macroscopic parameters i.e., power, pulse duration, and penetration depth of a typical laser desorption experiment to the dynamics at the molecular level.

To observe the effects predicted by Garrison et al.[1−3] the expanding plume needs to be probed at a point in time and space at which the clusters exist. The mass spectrometer used in this work allowed the ionization laser beam to be located 50 $\mu$m above the surface, thus enabling the experimental observation of phenomena occurring in the early stages of the plume dynamics. The close proximity of the ionization laser focus to the surface allows the desorption event to be probed on a submicrosecond time scale.

A representative single-shot L2ToF mass spectrum of laser-desorbed chrysene-$d_{12}$, shown in Figure 1a, was obtained at a delay time of 0.4 $\mu$s. The desorption laser power density was 15 MW cm$^{-2}$ with the post-ionization laser focused to $\sim$100 $\mu$m from the sample surface. The parent ion envelope consists of the molecular ion ($m/z = 240$), the $^{13}$C isotopomer ($m/z = 241$) and satellite [M-nD] peaks associated with the loss of 1$-$4 deuterium atoms from the parent chrysene-$d_{12}$. Each peak of the parent ion envelope is resolved to baseline ($m/\Delta m \sim 700$). These spectral features have been observed previously[23,24] in

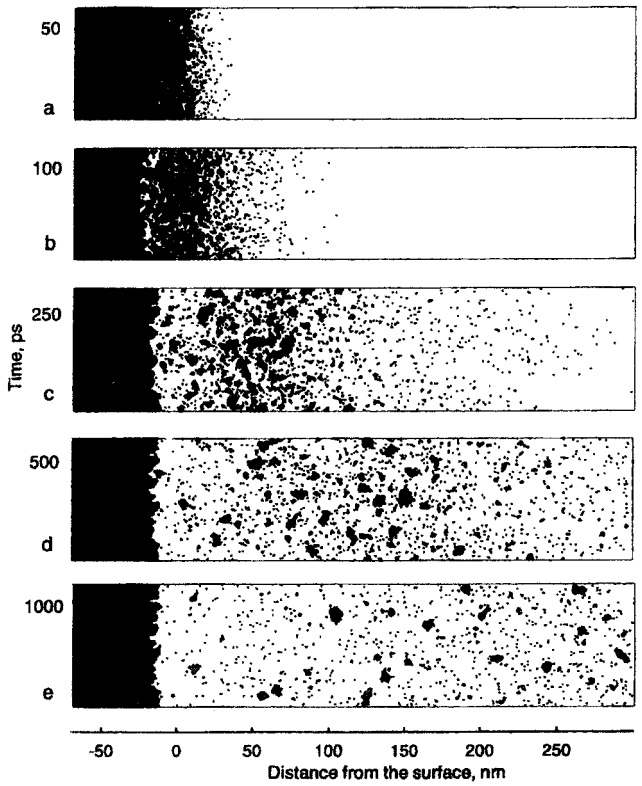


**Figure 3.** Simulated composition of a laser-desorption plume exhibiting clusters and discrete molecules. (Reproduced with permission from ref 3.)

laser ionization and standard electron impact mass spectra[25] of chrysene and are indicative of molecular ionization in the gas phase.

A significant broadening of each peak within the parent ion envelope was observed when the ionization laser focus was moved to a distance of 50 $\mu$m from the surface, as shown in Figure 1b. Peak broadening leading to overlapping peaks is extensive, and individual peaks within the parent ion envelope are no longer apparent in the spectra. These observations suggest that the ionization event is spatially and/or temporally expanded in contrast to that of ionization of molecules within the laser focus.

Consideration has to be given to the ionization of clusters upon irradiation, possibly leading to multiply charged clusters. Such clusters may diminish in size by evaporation of neutral molecules or charged species. For multiply charged clusters, a point is reached where the droplet diameter attains a critical size. At this point, the droplet becomes unstable and Coulombic repulsion leads to dispersion into smaller droplets.[26−28] As the laser-desorbed plume expands away from the surface, the repulsive evaporation of ions from multiply charged droplets enlarges the ionization volume. Furthermore, ionization of discrete molecules in a high density region of the plume also experience Coulombic repulsion following the extraction of the electrons by the static electric field. Consequently, these processes lead to the broadening of peaks and the reduction of mass resolution by space−charge effects. The contribution of space−charge effects arising solely from a high density of discrete gas phase ions cannot be entirely discounted. However, the estimated density of ions in the ionization focus[29] is well below the critical density threshold for space−charge effects determined by Villeneuve et al.[30]

We take as our starting point the premise that under the conditions employed here, the desorption plume comprises clusters of varying sizes along with individual molecules, as depicted in Figure 3. Mass spectra exhibiting features associated with the molecular cluster phenomena were observed at both extremes of laser desorption power density. The data presented in Figure 2 illustrate the time dependence of the cluster phenomena as a function of desorption laser power density for ionization at a fixed distance of 100 $\mu$m from the surface. Under conditions of low desorption power density, the size and/or number density of clusters was small and the clusters evaporate rapidly to individual molecules. Therefore, the broad ion signals associated with cluster ionization were only observed at short delay times after desorption. After this time, high-resolution peaks resulting from molecular ionization were observed and arise from two possible sources: the evaporation of the slower components of the desorbed clusters and delayed molecular desorption from the laser irradiated "warm" surface. Under conditions of higher desorption power densities the clusters are larger, more numerous, and survive for a longer period of time before evaporating. Hence, longer delay times are required before the molecular ionization was observed. Vertical profiles through the data of Figure 2 illustrate the temporal dependence for the ionization of discrete molecules or clusters at a particular desorption laser power. Two distinct regimes were encountered, termed cluster and molecular ionization, along with a transition period where intermediate resolution peaks are observed. Figure 2 also illustrates that the delay times required to observe both the high-resolution peaks and the onset of broad cluster signals increase with the desorption laser power. Calculations of the average velocity, in the region of discrete molecular ionization, at a desorption power of 15 MW cm$^{-2}$ was ~500 m s$^{-1}$. Velocities of this magnitude have been reported in the molecular dynamics models of Garrison et al.[1−3,31,32]

Reports of velocity distributions of laser-desorbed species are frequently based on determinations made at distances, when stated, in excess of several millimeters or even centimeters from the surface.[12,13] At these distances, the transient nature of the clusters is no longer observable and the measured velocities are dominated by the macroscopic translational motion of the laser-desorbed plume of molecules. Subtle effects of the creation and evaporation of clusters can be observed in the early stages of plume expansion corresponding to positions close to the surface. At locations close to the surface, the time for complete evaporation is intimately linked to the dynamic processes occurring in the laser-irradiated solid and subsequent release of material at early stages of plume development.

When the ionization laser is focused at ~100 $\mu$m from the surface, the appearance of the mass spectra recorded as a function of time illustrates the events that occur following the initial desorption event. For example, at a power density of 30 MW cm$^{-2}$, the initial desorption of clusters occurred for 0.5−0.8 $\mu$s after which the ionization laser probed isolated molecules desorbing from the surface for up to 2 $\mu$s after the incident laser pulse. At the higher desorption laser power density of 180 MW cm$^{-2}$, the cluster behavior was observed 1.0−1.5 $\mu$s after the initial desorption laser pulse, with isolated molecules only being observed to desorb from the surface after 1.5 $\mu$s. With higher incident energy and increased penetration depth, the number density and size of clusters are expected to increase. Only after the removal of clusters from the ionization region will the discrete molecules continuing to desorb from the surface be observed. Furthermore, the constant time difference of 0.4 $\mu$s between the onset of clustering and the time for maximum signal intensity, as shown in Figure 2, was observed for all laser power densities between 30 and 200 MW cm$^{-2}$. This trend indicates

that the time taken for the clusters to evaporate is independent of the laser power density.

The nanosecond laser desorption of neutral organic molecules from a solid sample is principally governed by the thermal properties of the solid and the absorbed laser energy. Comparison of the laser energy incident on the sample from a single desorption laser pulse (100 nJ) with the enthalpy of sublimation ($\Delta H_{sub}$) for chrysene (1800 nJ) indicates that there is insufficient laser energy to enact complete desorption of discrete molecules to the gas phase. This situation was recognized in Garrison's model[3] and supported the collective ejection of clusters. This process describes the ablation of the entire irradiated surface region on a macroscopic scale leading to the prediction of clusters in the desorption plume. The model uses 337 nm laser radiation of 15 ps duration and an optical penetration depth into the solid (molar mass = 100 Da) of 7 nm. The ablation process displaces the entire surface region at an average velocity of $\sim$200 ms$^{-1}$. The model predicts the onset of the desorption of droplets, termed collective ejection, at an energy density of $\sim$0.7 mJ cm$^{-2}$. This is equivalent to $\sim$50 MW cm$^{-2}$ for a 15 ps pulse. The highest power density simulated was $\sim$100 MW cm$^{-2}$ at which 20% of the ablation yield was said to consist of clusters. Because of computing restrictions, the model only extended to $\sim$0.3 $\mu$m away from the surface. However, clusters were still observed at this limit.

The phenomenon observed in this study is consistent with the formation of molecular clusters. Subsequent irradiation of an inhomogeneous mixture of molecules and clusters leads to the reduced resolution of the mass spectra. The desorption power density (15$-$180 MW cm$^{-2}$) and desorption depth ($\sim$400 nm) employed in this study differ from the data adopted by Garrison's picosecond model[3] (26$-$84 MWcm$^{-2}$, $\sim$30 nm desorption depth). However, it is feasible that the clusters of chrysene-$d_{12}$ could travel at least 50 $\mu$m before undergoing complete evaporation. The range of desorption laser power densities (15$-$180 MW cm$^{-2}$) is consistent with the predicted threshold for collective ejection. The phenomenon was observed over the entire range of desorption laser power densities used in this study.

Finally, laser desorption, the basis of the MALDI process,[33] is being used extensively in mass spectrometry to volatilize large molecules, including high mass biomolecules, into the gas phase. Intimate contact between the analyte and matrix molecules in the gas phase, perhaps within clusters, is believed[34] to be essential for ionization to occur. Hence, an understanding of the mechanism of laser desorption processes, including MALDI, clearly depends on identifying early events occurring in the plume leading to ion formation.

**Acknowledgment.** S.M.H. gratefully acknowledges the support of Heriot-Watt University for the award of a postgraduate studentship and Edinburgh Surface Analysis Technology for financial assistance and access to equipment.

## References and Notes

(1) Zhigilei, L. V.; Kodali, P. B. S.; Garrison, B. J. *Chem. Phys. Lett.* **1997**, *276*, 269.

(2) Zhigilei, L. V.; Kodali, P. B. S.; Garrison, B. J. *J. Phys. Chem. B* **1997**, *101*, 2028.

(3) Zhigilei, L. V.; Kodali, P. B. S.; Garrison, B. J. *J. Phys. Chem. B* **1998**, *102*, 2845.

(4) Itina, T. E.; Tokarev, V. N.; Marine, W.; Autric, M. *J. Chem. Phys.* **1997**, *106*, 8905.

(5) McCarthy, M. I.; Peterson, K. A.; Hess, W. P. *J. Phys. Chem.* **1996**, *100*, 6708.

(6) Philippoz, J.-M.; Zenobi, R.; Zare, R. N. *Chem. Phys. Lett.* **1989**, *158*, 12.

(7) Fain, B.; Lin, S. H.; Grotemeyer, J.; Schlag, E. W. *Chem. Phys. Lett.* **1993**, *202*, 357.

(8) Spengler, B.; Karas, M.; Bahr, U.; Hillenkamp, F. *J. Phys. Chem.* **1987**, *91*, 6502.

(9) Yang, M.; Reilly, J. P. *J. Phys. Chem.* **1990**, *94*, 6299.

(10) Li, Y.; McIver, R. T.; Hemminger, J. C. *J. Chem. Phys.* **1990**, *93*, 4719.

(11) Kinsel, G. R.; Lindner, J.; Grotemeyer, J.; Schlag, E. W. *J. Phys. Chem.* **1991**, *95*, 7824.

(12) Schilke, D. E.; Levis, R. J. *Rev. Sci. Instrum.* **1994**, *65*, 1903.

(13) Srinivasan, J. R.; Romano, L. J.; Levis, R. J. *J. Phys. Chem.* **1995**, *99*, 13272.

(14) Winter, B.; Mitzner, R.; Kusch, Ch.; Campbell, E. E. B.; Hertel, I. V. *J. Chem. Phys.* **1996**, *104*, 9179.

(15) Maechling, C. R.; Clemett, S. J.; Engelke, F.; Zare, R. N. *J. Chem. Phys.* **1996**, *104*, 8768.

(16) Balzer, F.; Gerlach, R.; Manson, J. R.; Rubahn, H.-G. *J. Chem. Phys.* **1997**, *106*, 7995.

(17) Elam, J. W.; Levy, D. H. *J. Chem. Phys.* **1997**, *106*, 10368.

(18) Elam, J. W.; Levy, D. H. *J. Phys. Chem. B* **1998**, *102*, 8113.

(19) Puretzky, A. A.; Geohegan, D. B. *Appl. Surf. Sci.* **1998**, *127*−*129*, 248.

(20) Muramoto, J.; Nakata, Y.; Okada, T.; Maeda, M. *Appl. Surf. Sci.* **1998**, *127*−*129*, 373.

(21) Nakata, Y.; Soumagne, G.; Okada, T.; Maeda, M. *Appl. Surf. Sci.* **1998**, *127*−*129*, 650.

(22) Murakami, K.; Makimura, T.; Ono, N.; Sakuramoto, T.; Miyashita, A.; Yoda, O. *Appl. Surf. Sci.* **1998**, *127*−*129*, 368.

(23) Hankin, S. M.; John, P.; Simpson, A. W.; Smith, G. P. *Anal. Chem.* **1996**, *68*, 3238.

(24) Hankin, S. M.; John, P.; Smith, G. P. *Anal. Chem.* **1997**, *69*, 2927.

(25) The standard EI mass spectrum of chrysene can be viewed at the NIST Webbook: http://webbook.nist.gov/chemistry/

(26) Hamdan, M.; Curcuruto, O. *Int. J. Mass Spec. Ion Proc.* **1991**, *108*, 93.

(27) Kebarle, P.; Tang, L. *Anal. Chem.* **1993**, *65*, 972A.

(28) Bruins, A. P. *J. Chrom. A* **1998**, *794*, 345.

(29) The profile of the laser craters and thus the ablated volume were determined using an atomic force microscope (Topometrix Accurex). Typical diameters of the laser-irradiated samples were in the range of 1$-$2 $\mu$m. From these measurements, approximately 100 fg of chrysene was desorbed per laser shot at a laser power of 15 MW cm$^{-2}$. The plume volumes, determined from the plume limits that yielded ions which were successfully detected, were estimated to be $6 \times 10^{-11}$ m$^3$. Assuming a uniform distribution of molecules throughout the plume and 100% ionization, the density of ions in the focal volume ($9 \times 10^{-14}$ m$^3$) was estimated to be $4 \times 10^{12}$ cm$^{-3}$. This represents the maximum density and, although subject to significant error associated with the heterogeneous composition of the plume and the ionization efficiency, it is believed to be below the critical density for space$-$charge effects.

(30) Villeneuve, D. M.; Fischer, I.; Zavriyev, A.; Stolow, A. *J. Chem. Phys.* **1997**, *107*, 5310.

(31) Zhigilei, L. V.; Garrison, B. J. *Appl. Phys. Lett.* **1997**, *71*, 551.

(32) Zhigilei, L. V.; Garrison, B. J. *Rap. Comm. Mass Spec.* **1998**, *12*, 1273.

(33) Dreisewerd, K.; Schurenberg, M.; Karas, M.; Hillenkamp, F. *Int. J. Mass Spec. Ion Proc.* **1995**, *141*, 127.

(34) Olumee, Z.; Vertes, A. *J. Phys. Chem. B* **1998**, *102*, 6118.